The Astrophysical Journal, 697:601–609, 2009 May 20 doi:10.1088/0004-637X/697/1/601

IS HO_2^+ A DETECTABLE INTERSTELLAR MOLECULE?

Susanna L. Widicus Weaver[1,4], David E. Woon[2], Branko Ruscic[3], and Benjamin J. McCall[1]
[1] Departments of Chemistry and Astronomy, University of Illinois at Urbana-Champaign, Urbana, IL 61801, USA; susanna.widicus.weaver@emory.edu, bjmccall@uiuc.edu
[2] Department of Chemistry, University of Illinois at Urbana-Champaign, Urbana, IL 61801, USA; davidewoon@gmail.com
[3] Chemical Sciences and Engineering Division, Argonne National Laboratory, Argonne, IL 60439, USA; ruscic@anl.gov
Received 2008 July 22; accepted 2009 March 5; published 2009 May 4

ABSTRACT

Although molecular oxygen, O_2, has long been thought to be present in interstellar environments, it has only been tentatively detected toward one molecular cloud. The fractional abundance of O_2 determined from these observations is well below that predicted by astrochemical models. Given the difficulty of O_2 observations from ground-based telescopes, identification of a molecule that could be used as a tracer of O_2 in interstellar environments would be quite useful. To this end, we have undertaken a collaborative examination of HO_2^+ in an attempt to evaluate the feasibility of its detection in interstellar clouds. We have conducted high-level ab initio calculations of its structure to obtain its molecular parameters. The reaction responsible for the formation of HO_2^+ is nearly thermoneutral, and so a careful analysis of its thermochemistry was also required. Using the Active Thermochemical Tables approach, we have determined the most accurate values available to date for the proton affinities of O_2 and H_2, and the enthalpy, Gibbs energy, and equilibrium constant for the reaction $H_3^+ + O_2 \rightarrow HO_2^+ + H_2$. We find that while this reaction is endothermic by $50 \pm 9\ cm^{-1}$ at 0 K, its equilibrium is shifted toward HO_2^+ at the higher temperatures of hot cores. We have examined the potential formation and destruction pathways for HO_2^+ in interstellar environments. Combining this information, we estimate the HO_2^+ column density in dense clouds to be $\sim 10^9\ cm^{-2}$, which corresponds to line brightness temperatures of $\leqslant 0.2$ mK. If our results prove correct, HO_2^+ is clearly not a detectable interstellar molecule.

Key words: ISM: abundances – ISM: molecules

1. INTRODUCTION

Molecular oxygen, O_2, is a simple diatomic molecule thought to be prevalent in dense molecular clouds. Chemical models predict the O_2 fractional abundance to be $X(O_2) = N(O_2)/N(H_2) = (5\text{–}10) \times 10^{-6}$ in regions of high extinction (Goldsmith et al. 2000 and references therein). The weak magnetic dipole-allowed transitions of O_2 should be observable in such regions if this fractional abundance is correct, but direct observations are limited to space-based observatories because of atmospheric spectral interference. Sensitive O_2 searches were carried out toward a large number of molecular clouds with the *Odin* satellite and the *Submillimeter Wave Astronomy Satellite* (*SWAS*). Surprisingly, O_2 was only tentatively detected toward one molecular cloud, ρ Ophiuchus A (Larsson et al. 2007; Goldsmith et al. 2002). The *Odin* observations provide a limit on the O_2 fractional abundance of 5×10^{-8} (Larsson et al. 2007), and upper limits calculated for other sources indicate fractional abundances of $<3 \times 10^{-7}$ (Goldsmith et al. 2000). The discrepancy between the observed and predicted abundances of O_2 indicates that its interstellar chemistry is very poorly understood. Recent chemical modeling indicates that even adjustment of the O_2 formation rate cannot entirely account for this discrepancy (Quan et al. 2008). Additional observational investigations are needed for insight into O_2 chemistry in dense clouds.

Given the difficulties in direct observation of O_2, alternate approaches for studying simple oxygen-related chemistry must be considered. A closely chemically related molecule with a large dipole moment could serve as a tracer for the elusive O_2 molecule through the use of highly sensitive radioastronomical observations. Indeed, protonated molecular oxygen, HO_2^+, has been proposed as such an O_2 tracer (Herbst et al. 1977). H_3^+ is a likely and efficient source of protonation in interstellar clouds, and interstellar HO_2^+ would therefore form from proton transfer to O_2 by the reaction

$$H_3^+ + O_2 \rightarrow HO_2^+ + H_2. \quad (1)$$

This reaction is very nearly isoenergetic, and, based on the relatively large uncertainties in standard reference data (Hunter & Lias 2005), it could be either slightly endothermic or slightly exothermic. A recent report (Ruscic et al. 2006) has revised the absolute proton affinity of O_2 upward and improved its accuracy, bringing it very close to the value tabulated (Hunter & Lias 2005) for the proton affinity of H_2. However, in order to confidently and accurately determine the overall thermochemistry of Reaction (1), an additional careful simultaneous determination of both absolute and relative proton affinities of O_2 and H_2 is necessary. This information could then be used to evaluate the viability of HO_2^+ as a tracer for O_2 in interstellar clouds.

In addition to the uncertain thermodynamics of Reaction (1), no laboratory rotational spectrum is available for HO_2^+. Ab initio calculations reported by Robbe et al. (2000) are not sufficiently accurate to guide observational searches. A new study by Huang & Lee (2008) was performed at a level comparable in many ways to the calculations we report below, though we have treated some properties which they did not. In the laboratory, a high-resolution infrared spectroscopic search for the HO_2^+ ν_1 band was conducted at frequencies above 3100 cm^{-1}, but only lines arising from H_3O^+ and H_2O^+ were observed (Ho et al. 1991). Infrared predissociation spectra of rare gas complexes with HO_2^+ indicate that the ν_1 band origin for the free ion should lie in the 2980–3040 cm^{-1} region (Nizkorodov et al. 1997). It is likely, then, that a high-resolution infrared study of HO_2^+ in this

[4] Current address: Department of Chemistry, Emory University, Atlanta, GA 30322, USA.

frequency range could provide sufficient spectral information to guide observational searches.

The laboratory characterization and observational search for HO_2^+ should be straightforward, but a thorough understanding of interstellar HO_2^+ chemistry and an accurate prediction of the HO_2^+ molecular parameters are required. To this end, we have undertaken a multidisciplinary collaboration to investigate HO_2^+ from a theoretical and computational viewpoint. We present here high-level ab initio electronic energy calculations, an analysis of HO_2^+ formation thermochemistry, an examination of interstellar HO_2^+ chemistry, and an evaluation of the likelihood for detection of HO_2^+ in the interstellar medium.

2. AB INITIO CALCULATIONS FOR HO_2^+

Ab initio quantum chemical calculations were performed in order to predict values for rotational constants, vibrational frequencies, dipole moments, and other properties of HO_2 and HO_2^+. It is important to benchmark the accuracy that can be attained for HO_2, for which there is much experimental information, as a measure of the expected accuracy of our predictions for HO_2^+. Huang & Lee (2008) chose to benchmark their approach on H_2O, so it is difficult to assess their accuracy for treating HO_2^+.

Both single reference coupled cluster [RCCSD(T)] and multireference configuration interaction (MRCI) calculations were performed. Valence correlation consistent basis sets as large as aug-cc-pV5Z were used (Dunning 1989; Kendall et al. 1992), along with extra core–valence *sp* functions from the cc-pCVDZ set (Woon & Dunning 1995). This level of theory surpasses the accuracy of the study by Robbe et al. (2000), and we used larger basis sets than Huang & Lee (2008) for deriving our potentials. Robbe et al. (2000) generated quartic force fields for ground-state HO_2 and the three lowest-lying states of HO_2^+ at the MRCI/aug-cc-pVQZ′ level, where the prime indicates that the *g* functions on O and *f* functions on H were omitted. The shorthand notation AVXZ (where X = T (triple), Q (quadruple), or 5 (quintuple)) represents aug-cc-pVXZ valence-only basis sets, while AVXZ+CVDZ indicates sets with the additional core–valence functions used in all-electron calculations. Our largest calculations used 342 basis functions. With the exception of the zero-field splitting treatment, all calculations were performed with MOLPRO (Werner et al. 2002), which features the internally contracted MRCI method (Werner & Knowles 1988; Knowles & Werner 1988) and an efficient implementation of open-shell coupled cluster theory (Knowles et al. 1993; Watts et al. 1993). For the MRCI calculations, a standard full-valence complete active space (CAS) multiconfigurational self-consistent field (MCSCF) wavefunction was employed (Werner & Knowles 1985; Knowles & Werner 1985). The O $2s^2$ orbitals were not forced to be doubly occupied.

To maximize accuracy, we used the systematic nature of the correlation consistent basis sets to extrapolate as many quantities as possible to their estimated complete basis set (CBS) limits (using TZ, QZ, and 5Z results). In this work, total valence energies, equilibrium structural parameters, and harmonic frequencies were all amenable to this treatment. The rotation–vibration coupling constants, α, and anharmonic constants, X, could not be extrapolated directly, but they usually exhibited little change between the AVQZ and AV5Z levels. Once a CBS limit or large basis value was identified, most properties were adjusted with a small core–valence correction (usually at the QZ level) by taking the difference between the valence AVXZ and all-electron AVXZ+CVDZ values.

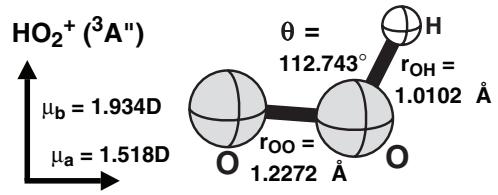

Figure 1. Equilibrium structural parameters for HO_2^+ (RCCSD(T) at the valence complete basis set limit with core–valence corrections) and dipole moment components (MRCI/AV5Z).

Table 1
Molecular Parameters Determined for HO_2 and HO_2^+

Spectroscopic Constant	HO_2 Calculated[a]	HO_2 Experimental[b]	HO_2^+ Calculated[a]
A_0 (GHz)	615.997	610.2733	659.301
B_0 (GHz)	33.604	33.5178	38.344
C_0 (GHz)	31.643	31.6677	35.885
ν_1 (cm^{-1})	3457	3436.2	3028
ν_2 (cm^{-1})	1406	1391.8	1440
ν_3 (cm^{-1})	1128	1097.6	1068
Δ_N (MHz)	0.1127	0.116908	0.1075
Δ_{NK} (MHz)	3.303	3.44572	5.515
Δ_K (MHz)	115.02	123.5906	299.03
μ_a (D)	1.405	1.412	1.518
μ_b (D)	1.572	1.541	1.934
D (cm^{-1})			6.870
E (cm^{-1})			0.033
ϵ_{aa} (MHz)	−46730	−49572	−1182
ϵ_{bb} (MHz)	−432	−422.9	−481
ϵ_{cc} (MHz)	−159	8.748	−476

Notes.
[a] This work.
[b] From Chance et al. (1997), Yamada et al. (1983), Burkholder et al. (1992), and Saito & Matsumura (1980).

Equilibrium structures were first optimized for various combinations of method and basis set. Anharmonic spectroscopic constants were then determined for most of those cases via perturbation theory analysis of potential energy surfaces. For each case, 84 energy calculations were run, representing the full sextic expansion of changes in the two bond lengths and the bond angle around the equilibrium structure. Step sizes were 0.1 a_0 for r_{OH} (1 a_0 = 0.529177 Å), 0.05 a_0 for r_{OO}, and 8° for θ. Bond length increments were 0, −1, +1, −2, +3, −3, and +5, while symmetric increments of 0, −1, +1, −2, +2, −3, and +3 were used for θ. Fitting and analysis were performed with SURFIT (Senekowitsch 1988) using a 69 term potential expanded in internal coordinates. In addition to the full quintic potential, sextic terms of types 600, 420, 330, and 222 were included. The rms fitting errors were <0.8 cm^{-1} in all cases and often $\leqslant 0.2$ cm^{-1}. The best equilibrium geometry is shown in Figure 1.

Some of the predictions for both HO_2 and HO_2^+ are given in Table 1, along with experimental data for HO_2. A detailed discussion of these results is presented in the following sections.

2.1. Reaction Energy and the Ground State of HO_2^+

Our computed prediction for the enthalpy of Reaction (1) at 0 K is 64.3 cm^{-1}, which includes anharmonic vibrational zero-point energy corrections (VZPE) and rotational zero-point energy corrections (RZPE). This result is the sum of the estimated valence CBS limit for the equilibrium reaction energy ΔE_e (+222.1 cm^{-1}) with a small correction for core–valence

contributions (+28.3 cm^{-1}), the harmonic VZPE (−199.5 cm^{-1}) and the anharmonic correction to VZPE (+76.4 cm^{-1}), and the RZPE (−63.0 cm^{-1}). Since computing the RZPE was beyond the scope of the present calculations, the last number is the sum of the experimental RZPE values for H_3^+ (64.121 cm^{-1}) and O_2 (−1.0857 cm^{-1}) from Lindsay & McCall (2001) and Cosby & Huestis (1992), respectively. While most of the contributions noted above are small in an absolute sense, they are clearly significant in light of the small final value of the reaction enthalpy.

As Robbe et al. (2000) noted, there is a very low-lying $^1A'$ state in the HO_2^+ system. They placed it just 1185 cm^{-1} (T_e) above the X^3A'' ground state at the MRCI/aug-cc-pVQZ′ level. We find a slightly larger value for T_e at the RCCSD(T) level (valence CBS limit) of 1391 cm^{-1}; the anharmonic VZPE correction increases the state separation by another 149 cm^{-1} (QZ level). While the ground state is unequivocally $^3A''$, the A^1A' state is clearly very close.

2.2. Rotational Constants

The predicted rotational constants in Table 1 were determined by first taking valence RCCSD(T) calculations for the equilibrium structural parameters to the CBS limit, yielding values for r_{OO}, r_{OH}, and θ of 1.3270 Å, 0.9709 Å, and 104.°458 for HO_2 and 1.2295 Å, 1.0110 Å, and 112.°529 for HO_2^+. Core–valence contributions at the QZ level shift these to our recommended all-electron equilibrium parameters r_{OO}, r_{OH}, and θ of 1.3247 Å, 0.9701 Å, and 104.549° for HO_2 and 1.2272 Å, 1.0102 Å, and 112.743° for HO_2^+. These geometries yield respective A_e, B_e, and C_e predictions of 622.263, 33.950, and 32.194 GHz for HO_2 and 647.983, 38.586, and 36.417 GHz for HO_2^+. The values of A_0, B_0, and C_0 given in Table 1 result from subtracting the rotation–vibration constants, α, summed over the three normal modes for each principal axis. The net α shifts are computed by adding core–valence contributions from QZ calculations to the valence AV5Z values. The difference between our predictions and the experimental values (Chance et al. 1997) is under 100 MHz for B_0 and C_0, which is an improvement over Robbe et al. (2000). The error in A_0 is ∼5 GHz; this constant is extremely sensitive to small errors in the bond angle. The predicted values of A_0, B_0, and C_0 reported by Huang & Lee (2008) are 649.428, 38.136, and 35.846 GHz, respectively.

2.3. Other Spectroscopic Properties

The predicted fundamental frequencies in Table 1 were determined in a similar manner as the rotational constants. Harmonic frequencies ω_i were computed at the RCCSD(T) level by adding core–valence shifts (QZ level) to the valence CBS limits, resulting in respective values for the symmetric stretch, the bend, and the asymmetric stretch of 1152, 1451, and 3671 cm^{-1} for HO_2 and 1104, 1459, and 3241 cm^{-1} for HO_2^+. The sum of the anharmonic constants for each mode was added to yield the values in Table 1 (valence AV5Z values with QZ core–valence adjustments). The stretches are both about 30 cm^{-1} too large for HO_2, while the bend is about 15 cm^{-1} too large. Interestingly, the prediction of 3028 cm^{-1} for ν_1 of HO_2^+ falls within the range suggested by Nizkorodov et al. (1997). The predicted values of ν_1, ν_2, and ν_3 reported by Huang & Lee (2008) are 3022, 1379, and 1058 cm^{-1}, respectively.

RCCSD(T)/AV5Z values for the centrifugal distortion constants are given in Table 1 and compared with experimental values of Chance et al. (1997) for HO_2. The errors for Δ_N and Δ_{NK} are <3 MHz, while the error in Δ_K exceeds 8 MHz.

The dipole moment values reported in Table 1 were determined at the MRCI/AV5Z level. The μ_a component is roughly parallel to the OO bond axis, while μ_b is dominated by the OH bond. The errors with respect to the experimental values of Saito & Matsumura (1980) for HO_2 are very small, just 0.008 D for μ_a and 0.031 D for μ_b. Our predictions for HO_2^+ are expected to be equally reliable. Both dipole moment components of HO_2^+ are larger than those of HO_2, which will lead to correspondingly more intense rotational transitions for the cation.

The lines of a triplet species such as HO_2^+ are split from magnetic interactions involving its two unpaired electrons, even in the absence of an applied field. The resulting zero-field splitting (ZFS) is customarily described in terms of the D and E tensors. The ORCA program (Neese 2008) was used to compute the spin–spin (SS) and spin–orbit coupling (SOC) contributions to the tensors (Ganyushin & Neese 2006), with the former computed at the CASSCF/AVQZ level and the latter at the MRCI/VQZ level and summed over the four lowest singlet and triplet states. Ground-state O_2 was used for benchmarking, and D_{SS} and D_{SOC} were computed to be 1.555 and 2.220 cm^{-1}, respectively, yielding a net computed D value of 3.775 cm^{-1}. This is within 0.2 cm^{-1} of the experimental value of 3.96 cm^{-1} (Tinkham & Strandberg 1955). See Ganyushin & Neese (2006) and Neese (2007) for additional ORCA benchmarks on O_2 and other species. For HO_2^+, the computed values of D_{SS} and D_{SOC} are 1.810 and 5.060 cm^{-1}, respectively, yielding a net of 6.870 cm^{-1} for D, almost twice the value for O_2. The value of E is 0.033 cm^{-1}.

The diagonal spin-rotation constants $\epsilon_{\alpha\alpha}$ of HO_2^+ were computed according to the expression given by Equation (2) of Barnes et al. (1978):

$$\epsilon_{\alpha\beta} \simeq -4B_\alpha \sum_{n\neq 0}{}' \langle 0|L_\alpha|n\rangle\langle n|\zeta_\beta L_\beta|0\rangle/(E_0 - E_n), \qquad (2)$$

where B_α is the rotational constant for axis α, $\zeta_\beta L_\beta$ represents the spin–orbit interaction on axis β, and E_0 and E_n are the energies of the electronic states $|0\rangle$ and $|n\rangle$, respectively. Barnes et al. (1978) deduced $\zeta_\beta L_\beta \sim \zeta L_\beta$ and $\zeta = 151$ cm^{-1}, and this value was employed along with the predicted rotational constants from Table 1. State separations were computed at the MRCI/AVTZ level, while the angular momentum matrix elements were computed at the CASSCF/AVTZ level. Predictions at the AVDZ level are very similar. The resultant values for HO_2 and HO_2^+ are given in Table 1. For HO_2, we summed over the four lowest-lying states of $^2A''$ and $^2A'$ symmetry. The ϵ_{cc} constant depends only on contributions within the $^2A''$ manifold, while ϵ_{aa} and ϵ_{bb} depend only upon matrix elements of the X^2A'' state with the $^2A'$ manifold. As one can see, agreement with the experimental values of Chance et al. (1997) varies from 2% for ϵ_{bb} to 6% for ϵ_{aa} to 1700% for ϵ_{cc}. For HO_2^+, we summed over the six lowest states of $^3A''$ and $^3A'$ symmetry. The predictions for ϵ_{bb} and ϵ_{cc} are the same order of magnitude as the same parameters for HO_2, but ϵ_{aa} is roughly a factor of 40 smaller. It is the largest of the three parameters in both cases since it depends upon A_0; it is particularly large for HO_2 because there is a very large contribution from the lowest-lying $^2A'$ state.

3. THERMOCHEMISTRY OF HO_2^+

The thermochemistry of Reaction (1), the proton transfer between H_2 and O_2, is dictated by the relative preference of the proton to be bound to each molecule. This can be quantified by comparing two closely related thermodynamic quantities, the

proton affinities (PA) and gas-phase basicities (GB) of molecular hydrogen and oxygen, which are defined by the reactions

$$H_2 + H^+ \rightarrow H_3^+ \quad (3)$$

$$O_2 + H^+ \rightarrow HO_2^+ \quad (4)$$

where $PA(H_2) = -\Delta_r H^\circ$(Reaction 3), $PA(O_2) = -\Delta_r H^\circ$ (Reaction 4), $GB(H_2) = -\Delta_r G^\circ$(Reaction 3), and $GB(O_2) = -\Delta_r G^\circ$(Reaction 4). Thus, the reaction enthalpy of Reaction (1) is $\Delta_r H^\circ(1) = PA(H_2)–PA(O_2)$ and the change in the Gibbs (or free) energy for Reaction (1) is $\Delta_r G^\circ(1) = GB(H_2)–GB(O_2)$.

In order to examine the thermochemistry of Reaction (1) in greater detail and obtain the best currently available estimate of its endothermicity/exothermicity ($\Delta_r H^\circ$) and endergonicity/exergonicity ($\Delta_r G^\circ$), particularly at the lower temperatures of interest in astrochemistry, we have employed the recently introduced Active Thermochemical Tables (ATcT) approach (Ruscic 2004; Ruscic et al. 2004, 2005a, 2006). This approach allows us to utilize the respectable body of knowledge on the *relative* PA and GB of H_2 and O_2 in a consistent manner and complement it with other pertinent determinations that directly or indirectly influence the *absolute* values of these parameters.

The ATcT results presented here are based on the most current version (1.068) of the Core (Argonne) Thermochemical Network [C(A)TN]. C(A)TN is the central TN from which ATcT derives its thermochemical knowledge. This TN is under continuous development and expansion; the current version encompasses nearly 900 chemical species containing H, O, C, N, and halogens, intertwined by about 10,000 thermochemically relevant determinations.

3.1. Previous Studies and Information Included in the ATcT

The Gibbs energies for Reaction (1) determined in previous experimental studies are summarized in Table 2 and were included in the ATcT analysis. While the enthalpy (as opposed to the Gibbs energy) of Reaction (1) cannot be inferred directly from these measurements (without introducing external estimates of the reaction entropy), the measurements imply that Reaction (1) is slightly exergonic at room temperature, in spite of the significant spread in values and substantial uncertainties. The slight exergonicity is encouraging in the context of interstellar chemistry, as this would strengthen the possibility that HO_2^+ is detectable.

In addition to the experimental studies of the Gibbs energy of Reaction (1), out of the remaining ∼10,000 determinations included in the current C(A)TN, of relevance to the present thermochemical results are those that link one or more species in Reaction (1) to the other species described by the TN and hence potentially contribute to the consensus values for $PA(O_2)$ and $PA(H_2)$. A detailed critical analysis of the underlying measurements or computations is outside the scope of this article, but we should mention that the ATcT analysis includes the experimental data related to $D_0(H_3^+)$ obtained by Cosby & Helm (1988a, 1988b), Dodhy et al. (1988), Helm (1988), Galster et al. (2001, 2005), and Ketterle et al. (1989); the theoretical determinations related to the stability of H_3^+ by Cencek et al. (1995, 1998), Röhse et al. (1993, 1994), Anderson (1992), Lie & Frye (1992), Frye et al. (1990), Jaquet & Röhse (1995), Jaquet et al. (1998), Polyansky & Tennyson (1999), Polyansky et al. (2000), Ramanlal et al. (2003), Mátyus et al. (2007), and Viegas et al. (2007); the determination of the relative PA of H_2 and OH by Cotter et al. (1972); and a number of experimental data related to the stability of HO_2^+ and HO_2, such as the ionization energy of HO_2 obtained by Litorja & Ruscic (1998); kinetic measurements by Srinivasan et al. (2006); the newer theoretical results on HO_2 obtained by Feller & Peterson (2007), Martin & de Oliveira (1999), Parthiban & Martin (2001), Boese et al. (2004), and Karton et al. (2006), as well as a number of determinations relevant to HO_2 as discussed and analyzed in detail in Ruscic et al. (2006).

Table 2
Experimental Results for the Gibbs Energy of Reaction (1)

$\Delta_r H^\circ_{298}$ [a] (kJ mol^{-1})	$\Delta_r G^\circ_{298}$ [a] (kJ mol^{-1})	Reference
−0.16 ± 0.57	0.13 ± 0.57	Fennelly et al. (1973)
	−1.5 ± 1.4	Fehsenfeld et al. (1975)
	−2.1 ± 1.9	Fehsenfeld et al. (1975)
−2.0 ± 1.0	−1.7 ± 1.0	Kim et al. (1975)
0.0 ± 0.15	−3.0 ± 1.5	Hiraoka et al. (1979)
1.4 ± 3.3	−1.7 ± 1.5	Bohme et al. (1980)
1.4 ± 0.3	−1.48 ± 0.49	Adams & Smith (1984)
1.3 ± 11	−1.6 ± 11	Hunter & Lias (2005)

Note.
[a] Uncertainties are 2σ values in lieu of 95% confidence limits (which is the standard practice for the expression of uncertainties in thermochemistry). While the listed ΔG values can be obtained solely from the measured quantities and were utilized in the ATcT analysis, the listed ΔH values are not measured quantities (with one exception; Adams & Smith 1984). Rather, they have been inferred by the original authors through external estimates of the reaction entropy and are given here only for the sake of completeness. Also note that the value from Hunter & Lias (2005) is a prior evaluation, listed only for the purpose of comparison.

Table 3
Results for H_2 and O_2 Obtained from the ATcT Analysis

Thermochemical Quantity	H_2 [a] (kJ mol^{-1})	O_2 [a] (kJ mol^{-1})
PA_{298}	423.351 ± 0.012	422.04 ± 0.11
GB_{298}	395.953 ± 0.012	397.70 ± 0.11
$PA_0 = GB_0$	417.780 ± 0.012	417.18 ± 0.11

Note. [a] Uncertainties reflect 95% confidence limits.

3.2. ATcT Results for $PA(H_2)$, $PA(O_2)$, and the Thermochemistry of $H_3^+ + O_2 \rightarrow HO_2^+ + H_2$

The final ATcT results for PA and GB of H_2 and O_2 are given in Table 3, and those for Reaction (1) are given in Table 4. The reported thermochemistry is the most accurate to date, showing that the formation of HO_2^+ is, in fact, slightly endothermic at all temperatures. However, while the reaction starts as endergonic at 0 K, it becomes ergononeutral at ∼130 K, and at 298.15 K is clearly exergonic. These trends are shown more clearly in Table 5, which is a JANAF-style tabulation that provides a more detailed account of the temperature dependence of the enthalpy, Gibbs energy, entropy ($\Delta_r S^\circ_T$), and equilibrium constant (K_T) of Reaction (1).

4. PARTITION FUNCTIONS AND EQUILIBRIUM CONSTANT

For the purpose of relating different thermochemical measurements in the ATcT calculations, it is necessary to compute the internal partition function of the four molecules in Reaction (1). These partition functions are also necessary for the evaluation of the equilibrium constant of Reaction (1), which

Table 4
Thermochemical Results for Reaction (1) Obtained from the ATcT Analysis

Thermochemical Quantity	kJ mol^{-1} [a]	cm^{-1} [a]
$\Delta_r H^\circ_0$	0.60 ± 0.11	50 ± 9
$\Delta_r H^\circ_{298}$	1.31 ± 0.11	110 ± 9
$\Delta_r G^\circ_0$	0.60 ± 0.11	50 ± 9
$\Delta_r G^\circ_{298}$	−1.75 ± 0.11	−146 ± 9

Note. [a] Uncertainties reflect 95% confidence limits.

Table 5
JANAF-Style Tabulation of the Thermochemical Properties of Reaction (1)

T (K)	$\Delta_r S^\circ_T$ (J mol^{-1} K^{-1})	$[H^\circ_T - H^\circ_0]_r$ (kJ mol^{-1})	$\Delta_r H^\circ_T$ (kJ mol^{-1})	$\Delta_r G^\circ_T$ (kJ mol^{-1})	$\log_{10}[K_T]$
0	0.000	0.000	0.601	0.601	−∞
5	−5.758	0.007	0.609	0.638	−6.6604
10	−4.939	0.013	0.614	0.663	−3.4647
20	−4.955	0.013	0.614	0.713	−1.8627
40	0.130	0.177	0.779	0.773	−1.0099
50	3.805	0.342	0.944	0.753	−0.7869
60	6.652	0.498	1.099	0.700	−0.6095
80	9.722	0.708	1.309	0.532	−0.3471
100	10.775	0.801	1.402	0.325	−0.1695
120	10.986	0.823	1.424	0.106	−0.0462
140	10.876	0.808	1.410	−0.113	0.0421
150	10.778	0.794	1.396	−0.221	0.0770
160	10.674	0.778	1.379	−0.328	0.1072
180	10.476	0.745	1.346	−0.540	0.1567
200	10.322	0.715	1.317	−0.748	0.1953
250	10.164	0.681	1.282	−1.259	0.2630
298.15	10.258	0.708	1.309	−1.749	0.3065
300	10.266	0.710	1.311	−1.768	0.3079
350	10.533	0.797	1.399	−2.288	0.3414
400	10.893	0.933	1.534	−2.823	0.3687

affects the expected abundance of HO_2^+ in interstellar clouds (described in Section 5). In this section, we describe the method of calculation of the partition functions in the ATcT, the calculation of the equilibrium constant, and the effect of nuclear spin selection rules.

4.1. Evaluation of Partition Functions

For all four species of interest, internal partition functions have been calculated by direct level counting using the usual formula

$$q_{\rm int} = \sum_i g_J g_I e^{-\frac{E_i}{kT}} \quad (5)$$

where i labels all rovibronic states of the molecule below 10,000 cm^{-1}, g_J is each state's rotational and electronic degeneracy, g_I its nuclear spin degeneracy, and E_i its energy. We follow the standard thermochemical convention of renormalizing the partition functions by the total nuclear spin degeneracy, $\Pi_j(2I_j + 1)$, where j indexes the nuclei and I_j are their nuclear spins. For example, for H_2 we take $g_I = \frac{1}{4}$ for para-H_2 and $\frac{3}{4}$ for ortho-H_2. The absence of such renormalization would adversely affect the resulting absolute entropies of the individual species and make them incompatible with those found normally in thermochemical tabulations. However, it should be noted that the absence of such renormalization would not affect the resulting equilibrium constant or the resulting Gibbs energy of the reaction, as long as the same convention is applied to all reactants and products. We also follow the essential convention of choosing the lowest *allowed* rotational level of the molecule (hereafter referred to as the "ground state") as the zero of the energy. We wish to emphasize that, as opposed to the renormalization of the partition function, adherence to the convention of choosing the lowest allowed level as the zero of the energy is very important, even though it is not always followed. For example, Sidhu et al. (1992) chose the forbidden $J = K = 0$ level of H_3^+ as their zero point, with the result that their calculated partition function took on a nonphysical value of 0 as $T \to 0$.

For H_3^+, we used the experimentally determined energy levels from Lindsay & McCall (2001; offset so that the $J = K = 1$ level is at $E = 0$), and supplemented these with estimates of the few missing levels up to our 10000 cm^{-1} cutoff based on their reported spectroscopic constants. The renormalized nuclear spin degeneracy factors are $g_I = \frac{1}{2}$ for $G = 0$ (mod 3) and $\frac{1}{4}$ for $G \neq 0$ (mod 3).

For H_2, the relevant levels were taken from Gurvich et al. (1989, 1991, 1996; which are based on calculations of Waech & Bernstein 1967 and Le Roy 1971 that used the potential energy function of Kołos & Wolniewicz 1964, 1965, 1968). For O_2, the levels were computed from the spectroscopic constants in Huber & Herzberg (1979), and $g_I = 1$ for the levels symmetric with respect to nuclear permutation (odd J in $X^3\Sigma_g^-$) and 0 for the asymmetric levels. In the cases of both H_2 and O_2, the resulting partition function-related data matches exactly (within an occasional round-off error of 0.001 kJ mol^{-1}) the thermochemical data of Gurvich et al. (1989, 1991, 1996) (also obtained by direct counting, but given in tabular form with fixed increments), subsequently adopted as a canon by CODATA (Cox et al. 1989).

For HO_2^+, the relevant levels were computed during the initial investigations using the theoretically obtained spectroscopic constants of Robbe et al. (2000) for the X^3A'', a^1A', and b^1A'' states, and were in the later stages replaced with the theoretical spectroscopic constants given in Section 2. Our cutoff of 10,000 cm^{-1} includes a large number of vibrational levels, as well as both excited electronic states. Since HO_2^+ is a near-prolate rotor with a very small asymmetry factor, the levels above $J = 10$ were computed using the symmetric rotor approximation in order to lower the number of levels that ATcT needs to repeatedly count. We have separately verified that the prolate approximation for $J > 10$ does not introduce an error in the computed partition function-related quantities.

Figure 2 shows a plot of the calculated internal partition functions for the four chemical species involved in Reaction (1), over a temperature range of 2–300 K. Qualitatively, the ordering of these curves can be understood by the mass and complexity of the molecules. The oxygen-bearing molecules are considerably heavier than the pure hydrogenic species, so they have smaller rotational constants and more closely spaced energy levels. The linear molecules H_2 and O_2, which can be thought of as extremely prolate tops ($A \to \infty$) that are effectively restricted to $K = 0$, have fewer energy levels than the symmetric top H_3^+ or the asymmetric top HO_2^+.

4.2. Calculation of Equilibrium Constant

The equilibrium constant for Reaction (1) is defined as

$$K_T(1) = \frac{n(HO_2^+)n(H_2)}{n(H_3^+)n(O_2)}, \quad (6)$$

where n(X) is the number density of species X. From elementary statistical mechanics and thermodynamics, the

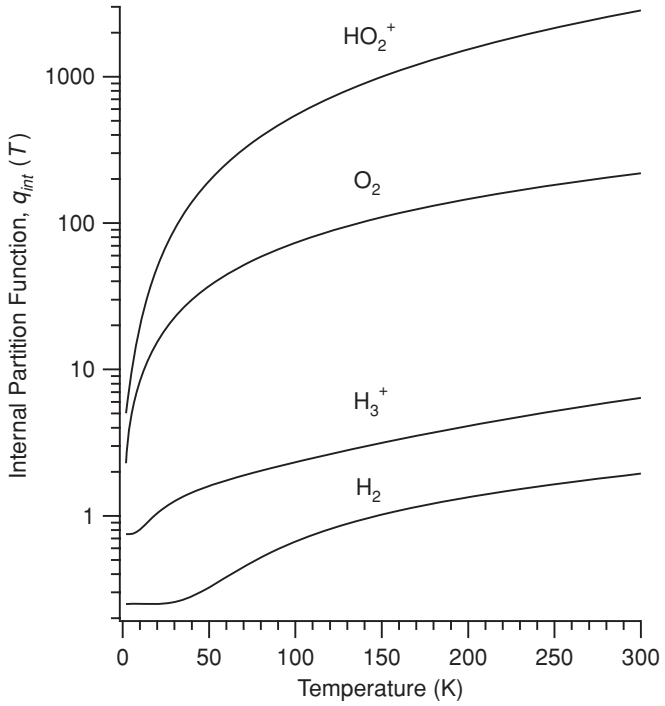

Figure 2. Calculated internal partition function $q_{\rm int}$ for the four molecules involved in Reaction (1) as a function of temperature. Note that the partition functions follow the conventions adopted in thermochemistry (see the text).

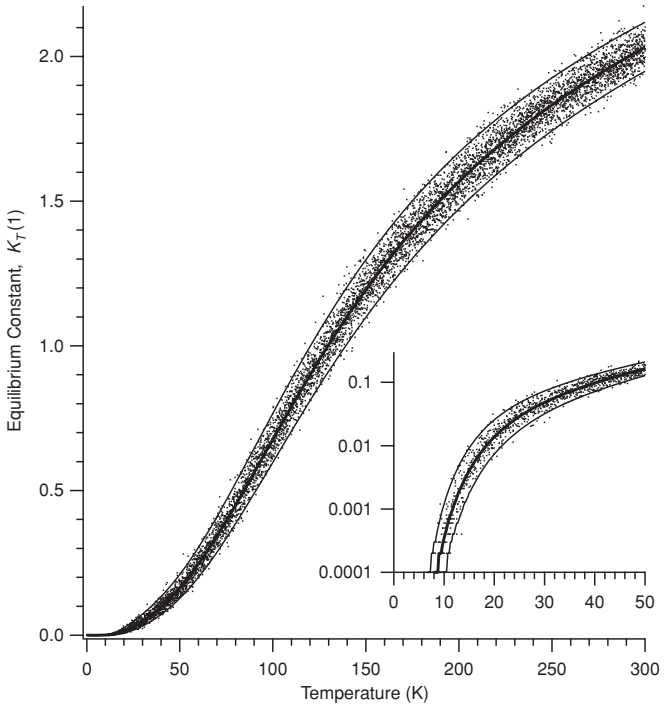

Figure 3. Equilibrium constant for Reaction (1) as a function of temperature. The thick line is the central value, the thin lines denote the upper and lower 95% confidence limits, and the points are a Monte Carlo sampling of the uncertainty spread. The low temperature values are shown with a logarithmic scale in the inset for clarity.

equilibrium constant is related to the Gibbs energy via $\ln K_T(1) = -\Delta_r G^\circ_T(1)/(RT)$, where R is the universal gas constant. Using additional basic relationships of thermodynamic quantities, the equilibrium constant can be expressed in the equivalent form

$$K_T(1) = e^{-\frac{E_0(1)}{kT}} \frac{q(\mathrm{HO_2^+})q(\mathrm{H_2})}{q(\mathrm{H_3^+})q(\mathrm{O_2})}, \quad (7)$$

where k is the Boltzmann constant and the reaction enthalpy $E_0(1)/k$ is equivalent to $\Delta_r H^\circ_0(1)/R$. The partition function q of any chemical entity, which depends on the temperature T, can be expressed as the product of the translational partition function, $q_{\rm tr}$, and the internal partition function, $q_{\rm int}$. The classical translational partition function is proportional to $m^{3/2}$, where m is the mass of the molecule. The ratio of the product of the translational partition functions of the products to that of the reactants is then simply $[m(\mathrm{HO_2^+})m(\mathrm{H_2})/m(\mathrm{H_3^+})m(\mathrm{O_2})]^{3/2} = 0.570$, where the present calculation of the numerical value uses the atomic weights from Audi et al. (2003) and assumes the most common isotopes. The final result is

$$K_T(1) = 0.570 e^{-\frac{E_0(1)}{kT}} \frac{q_{\rm int}(\mathrm{HO_2^+})q_{\rm int}(\mathrm{H_2})}{q_{\rm int}(\mathrm{H_3^+})q_{\rm int}(\mathrm{O_2})}. \quad (8)$$

Figure 3 shows the equilibrium constant for Reaction (1), calculated using Equation (8), over the range of 2–300 K, for the value of the reaction enthalpy obtained by ATcT. The thick line corresponds to the central value of $K_T(1)$, while the thinner lines above and below indicate the upper and lower bounds corresponding to the 95% confidence limits of the equilibrium constant. Comparison of the direct experimental determinations of the equilibrium constant of Reaction (1) (listed in Table 2 in the form of $\Delta_r G^\circ_{298}$ values) with the ATcT value $K_{298} = 2.025 \pm 0.085$ (or $\Delta_r G^\circ_{298} = -1.75 \pm 0.11$ kJ mol^{-1}) shows that all measurements are consistent, within their uncertainties, with the ATcT value, except for the earliest determinations, which were subsequently shown to be incorrect.

At low temperatures, the reverse reaction is strongly favored, while as the temperature grows the forward reaction dominates. This is due to entropy, as the density of states of $\mathrm{HO_2^+}$ grows fastest with temperature, favoring the products. It is interesting to examine these results in the context of typical interstellar conditions. At temperatures higher than ~130 K, such as are often encountered in hot cores, $K_T(1) > 1$ and the equilibrium is shifted toward $\mathrm{HO_2^+}$. At the temperatures of the diffuse interstellar medium (~60–100 K), $K_T(1)$ ranges from $\sim 0.246 \pm 0.052$ to 0.677 ± 0.085. At the even lower temperatures of cold dense clouds, the equilibrium constant is considerably smaller but also more uncertain in terms of relative error: $0.048^{+0.025}_{-0.016}$ at 30 K, $0.014^{+0.012}_{-0.007}$ at 20 K, and $0.00034^{+0.00086}_{-0.00024}$ at 10 K.

4.3. Nuclear Spin Selection Rules

The preceding analysis has neglected the effects of nuclear spin angular momentum selection rules in chemical reactions, and has treated Reaction (1) on a purely statistical thermodynamical basis. That is, it was assumed that a given pair of quantum states of the reactants could proceed to any quantum states of the products. However, as theoretically predicted by Quack (1977) and expanded on by Oka (2004), the conservation of the total nuclear spin angular momentum throughout a chemical reaction involving identical nuclei leads to selection rules on the final states of the products. These effects have been experimentally demonstrated in reactions involving $\mathrm{H_2^+}$ and $\mathrm{H_3^+}$ by Uy et al. (1997), Cordonnier et al. (2000), and Tom et al. (2008).

The branching fractions for the reverse of Reaction (1), $\mathrm{H_2 + HO_2^+ \rightarrow H_3^+ + O_2}$, are easily calculated using the angular

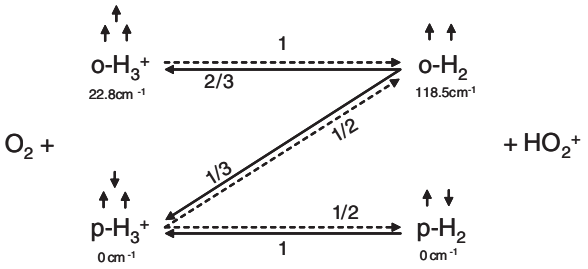

Figure 4. Branching fractions for the formation and destruction of HO_2^+ based on nuclear spin statistics. The energies do not include the reaction enthalpy.

momentum method of Oka (2004). The reaction of ortho-H_2 ($I = 1$) with HO_2^+ ($I = 1/2$) is represented as $\mathcal{D}_1 \otimes \mathcal{D}_{1/2}$, which using the angular momentum addition rules yields $\mathcal{D}_{3/2} \oplus \mathcal{D}_{1/2}$, corresponding to ortho-H_3^+ ($I = 3/2$) + O_2 ($I = 0$) and para-H_3^+ ($I = 1/2$) + O_2 ($I = 0$), respectively. Accounting for the statistical weights ($2I + 1$), this means that the branching fraction of ortho-H_3^+:para-H_3^+ is 4:2. For the reaction of para-H_2 with HO_2^+, $\mathcal{D}_0 \otimes \mathcal{D}_{1/2} = \mathcal{D}_{1/2}$, so only para-$H_3^+$ can be produced.

To evaluate the forward reaction $H_3^+ + O_2 \rightarrow H_2 + HO_2^+$, we must reverse the relations derived above. We note that ortho-H_3^+ ($\mathcal{D}_{3/2}$) can be produced only from $\mathcal{D}_1 \otimes \mathcal{D}_{1/2}$, and we can immediately infer that $\mathcal{D}_{3/2} \rightarrow 4(\mathcal{D}_1 \otimes \mathcal{D}_{1/2}/6)$, where the 4 and 6 balance the statistical weights. From a chemical perspective, this implies that the reaction of ortho-H_3^+ + O_2 can yield only ortho-H_2 + HO_2^+. To derive the branching fractions for para-H_3^+ + O_2 we can add the two relations of the previous paragraph to obtain $\mathcal{D}_{3/2} \oplus 2\mathcal{D}_{1/2} = (\mathcal{D}_1 \otimes \mathcal{D}_{1/2}) \oplus (\mathcal{D}_0 \otimes \mathcal{D}_{1/2})$ and then subtract the relation $\mathcal{D}_{3/2} \rightarrow 4(\mathcal{D}_1 \otimes \mathcal{D}_{1/2}/6)$ to find $\mathcal{D}_{1/2} \rightarrow (\mathcal{D}_1 \otimes \mathcal{D}_{1/2}/6) \oplus (\mathcal{D}_0 \otimes \mathcal{D}_{1/2})$. Thus, the reaction of para-H_3^+ with O_2 has a branching fraction of ortho-H_2:para-H_2 = 1:1.

The branching ratios determined from this analysis are shown schematically in Figure 4. The consequences of these selection rules on Reaction (1) are quite severe, in light of the fact that the lowest level of ortho-H_2 (the level $J = 1$) lies 118.5 cm^{-1} (170.5 K) above the $J = 0$ para-H_2 ground state. The reaction enthalpy of $\Delta H = 50 \pm 9$ cm^{-1} corresponds to the reaction of the ground state ($J = K = 1$) of para-H_3^+ with O_2 to produce para-H_2 and HO_2^+. Consequently, the reaction of para-H_3^+ with O_2 to form ortho-H_2 ($J = 1$) and HO_2^+ is endothermic by $\Delta H = 169 \pm 9$ cm^{-1}, which is quite a significant quantity. The reaction of the lowest state ($J = 1$, $K = 0$) of ortho-H_3^+ (22.8 cm^{-1} above $J = K = 1$) to form ortho-H_2 and HO_2^+ is endothermic by $\Delta H = 146 \pm 9$ cm^{-1}. In principle, the least endothermic reaction would be the that of ortho-H_3^+ with O_2 to form para-H_3^+ and HO_2^+. That reaction is, however, cast out by selection rules and does not occur.

Clearly, a more sophisticated treatment for calculating the equilibrium constant which takes these selection rules into account would be desirable. In the absence of such a treatment, we can still make a rough estimate of the impact of these selection rules by multiplying the equilibrium constant calculated from Equation (8) by a factor of $e^{-E_{\rm rot}/kT}$. In the case of the reaction of ortho-H_3^+ with O_2 (which can only make ortho-H_2), this factor is $e^{-96/kT}$; for a typical dense cloud temperature of ~30 K this is 1%, and for a hot core at ~100 K this is 25%. The equilibrium constant for the reaction of para-H_3^+ with O_2 to form ortho-H_2 must be multiplied by an even smaller factor $e^{-119/kT} \sim 18\%$ at 100 K.

For a crude estimate we can assume that these reactions are negligible, leaving only the reaction of para-H_3^+ with O_2 to form para-H_2, which is only half of the total reaction of para-H_3^+ with O_2. If we assume a H_3^+ ortho:para ratio of ~1 as observed in dense clouds (McCall et al. 1999), the rate of the forward Reaction (1) will be cut by a factor of 4 (2 from the loss of the ortho-H_3^+ reaction, and another 2 from the loss of half of the para-H_3^+ reaction). The rate of the reverse reaction is not much affected by the selection rules, since almost all H_2 is in the para form in dense clouds (Lacy et al. 1994), and this goes exclusively to para-H_3^+ which is the ground state. For the sake of argument, we assume that this is also the case for hot cores, as there is no information on the H_2 ortho:para ratio in these sources. We therefore crudely estimate $K_T(1)$ to be reduced by a factor of 4 at low temperatures. We wish to emphasize that a more sophisticated treatment would be desirable.

5. TESTING THE FEASIBILITY OF HO_2^+ OBSERVATIONAL SEARCHES

We have shown that the formation of HO_2^+ is an endothermic process, which greatly decreases the likelihood of its detection. However, its endothermic formation does not entirely preclude the presence of HO_2^+ in interstellar environments, especially in warmer environments, such as hot cores, where $K_T > 1$ for Reaction (1). In order to evaluate whether a dedicated observational search for HO_2^+ is warranted, we must first determine the feasibility of its detection.

A spectral prediction for HO_2^+ could be compared directly to available observational surveys, or could guide a dedicated observational search. Such a prediction could be produced from the information in Section 2, though the inclusion of spin–spin interactions for an asymmetric top significantly complicates this exercise. However, given the uncertainties in the A rotational constant (~5 GHz) and the D spin–spin parameter (~2 cm^{-1}, or 60 GHz), any prediction made at this time would have insufficient frequency accuracy for these purposes. Direct comparisons to observations therefore cannot be made until laboratory measurements are available. The results of Section 2 will be quite helpful in guiding these future laboratory studies.

Despite the lack of accurate frequency predictions, the line strengths of pure rotational transitions are well known. An estimate of the observational line brightness can therefore be made from this information. Observed line intensities will scale as $[K_T(1)/q_{\rm int}]e^{-E_u/kT}$, accounting for the temperature dependence of the equilibrium constant, the partition function, and the Boltzmann factor. From this information we find that line intensities will peak at temperatures near 100 K, and so hot cores are indeed the best sources for observational searches.

In addition to the optimum temperature, we must also calculate the expected interstellar abundance of HO_2^+ before the estimated line brightness can be determined. This calculation relies on evaluation of HO_2^+ formation and destruction mechanisms. In the interstellar medium, the most likely formation mechanism for HO_2^+ is Reaction (1). Three other potential formation mechanisms are listed in the UMIST Database (Woodall et al. 2007), but are likely to be considerably slower than Reaction (1). The first is the reaction of H_2^+ with O_2, which will be much slower than Reaction (1) because H_2^+ is much less abundant than H_3^+ due to the fast reaction of H_2^+ with H_2 to form H_3^+. The second is the reaction of NH^+ with O_2, which has a somewhat lower rate constant (1.6×10^{-10} cm^3 s^{-1}) and is also likely slower than Reaction (1), as NH^+ should be less abundant than H_3^+ (even in diffuse clouds, the neutral NH (Meyer & Roth 1991) is less

abundant than H_3^+). The third is the reaction between HCO and O_2^+ ($k = 3.6 \times 10^{-10}$ cm^3 s^{-1}), which is also likely to be much slower than Reaction (1); according to the dense cloud models of Lee et al. (1996), O_2^+ is roughly 5 orders of magnitude less abundant than O_2, and HCO is about 1 order of magnitude less abundant than H_3^+.

The UMIST database (Woodall et al. 2007) lists 24 potential destruction reactions for HO_2^+, but most of these involve species of low abundance. The three most significant are the reactions with H_2 (the inverse of Reaction (1)), with CO, and with an electron. The reaction with CO is a moderately fast Langevin reaction ($k = 8.4 \times 10^{-10}$ cm^3 s^{-1}) but cannot compete with the reaction with H_2 given that CO is roughly 4 orders of magnitude less abundant. The dissociative recombination reaction has a much higher rate coefficient ($k = 3.0 \times 10^{-7}$ cm^3 s^{-1}), but this reaction will still be slower than that with H_2 for the ionization fractions relevant to molecular gas (only $\sim 10^{-4}$ even in diffuse clouds).

Determination of the timescale for Reaction (1) reveals that the ratio of $n(HO_2^+)/n(H_3^+)$ achieves 99% of the equilibrium value in 3.8×10^6 s under typical dense cloud conditions. The steady state condition is therefore a valid assumption for calculating the expected HO_2^+ density in interstellar clouds. Equating the rate of formation with the rate of destruction, and incorporating the definition $k_1/k_{-1} = K_T(1)$, we find

$$n(HO_2^+) = \frac{k_1}{k_{-1}} n(H_3^+) \frac{n(O_2)}{n(H_2)} = K_T(1) n(H_3^+) \frac{n(O_2)}{n(H_2)} \quad (9)$$

which allows us to evaluate the likely interstellar abundance of HO_2^+. We note that the right hand side of this equation is equivalent to Equation (6), which implies that Reaction (1) is in equilibrium. The astrochemistry of HO_2^+ therefore represents an interesting and unusual case for interstellar chemistry where the assumption of steady state implies a true chemical equilibrium, because the dominant destruction reaction is the reverse of the dominant formation reaction.

Dense clouds, where H_3^+ has a number density $\sim 10^{-4}$ cm^{-3} (McCall 2006), are likely to harbor more HO_2^+ than diffuse clouds, where $n(H_3^+) \sim 10^{-6}$ cm^{-3} (Indriolo et al. 2007). If we assume that O_2 contains all of the oxygen not in the form of CO, then we would expect $n(O_2)/n(H_2) \sim 10^{-5}$, which is consistent with astrochemical models (Goldsmith et al. (2000) and references therein). However, we note that the results from *SWAS* (Goldsmith et al. 2002) and *Odin* (Larsson et al. 2007) suggest that the O_2/H_2 ratio can be substantially lower than this value.

Taking the value of $K_T(1)$ for 100 K from Table 5 and neglecting nuclear spin statistics, this yields a number density $n(HO_2^+) \sim 7 \times 10^{-10}$ cm^{-3}. In a cloud with line-of-sight pathlength of ~ 1 pc, this implies a column density $N(HO_2^+) \sim 2 \times 10^9$ cm^{-2}. Assuming a typical hot core linewidth of 10 km s^{-1}, this would correspond to line brightness temperatures of $\leqslant 0.2$ mK for all HO_2^+ lines at frequencies <1 THz. This frequency range corresponds to windows accessible by the current generation of ground-based radio telescopes, where the achievable noise level is generally >1 mK. Based on the assumptions outlined here, HO_2^+ is clearly not detectable in the interstellar medium with current receiver technology.

6. CONCLUSIONS

We have presented here the results of a multidisciplinary theoretical and computational analysis of HO_2^+ in an attempt to evaluate its feasibility as a tracer of O_2 in interstellar clouds. We have conducted high-level ab initio calculations of HO_2^+ to obtain its molecular parameters. This information can be used to guide laboratory studies, but is insufficiently accurate to guide observational searches. We have also examined the thermochemistry of the HO_2^+ formation mechanism, and from this determined that this process is endothermic by 50 ± 9 cm^{-1}. This endothermicity unfortunately renders HO_2^+ undetectable under typical interstellar conditions, with the predicted line intensities falling far below the detection levels of existing radiotelescope receivers.

Support for S.L.W.W. and B.J.M. was provided by an NSF CAREER award (NSF CHE-0449592) and the UIUC Critical Research Initiative program. D.E.W. acknowledges support by the NASA Exobiology program (NNX07AN33G); he also thanks Professor Kirk Peterson of Washington State University for providing the current version of SURFIT and for guidance regarding its use and interpretation of results; Professor Frank Neese of the University of Bonn for assistance with running ORCA; and Professor Thom H. Dunning, Jr. for computational resources. The work at Argonne National Laboratory was performed under the auspices of the Office of Basic Energy Sciences, Division of Chemical Sciences, Geosciences, and Biosciences, US Department of Energy, under contract DE-AC02-06CH11357. Portions of the research presented in this paper are part of ongoing work in the framework of a Task Group of the International Union of Pure and Applied Chemistry (IUPAC) on "Selected Free Radicals and Critical Intermediates: Thermodynamic Properties from Theory and Experiment" (IUPAC Project 2003-024-1-100; see Ruscic et al. 2005b for further details).

REFERENCES

Adams, N. G., & Smith, D. 1984, Chem. Phys. Lett., 105, 604
Anderson, J. B. 1992, J. Chem. Phys., 96, 3702
Audi, G., Wapstra, A. H., & Thibault, C. 2003, Nucl. Phys. A, 729, 337
Barnes, C. E., Brown, J. M., Carrington, A., Pinkstone, J., Sears, T. J., & Thistlethwaite, P. J. 1978, J. Mol. Spectrosc., 72, 86
Boese, A. D., Oren, M., Atasoylu, O., Martin, J. M. L., & Kállay M., Gauss, J. 2004, J. Chem. Phys., 120, 4129
Bohme, D. K., Mackay, G. I., & Schiff, H. I. 1980, J. Chem. Phys., 73, 4976
Burkholder, J. B., Hammer, P. D., Howard, C. J., Towle, J. P., & Brown, J. M. 1992, J. Mol. Spectrosc., 151, 493
Cencek, W., Komasa, J., & Rychlewski, J. 1995, Chem. Phys. Lett., 246, 417
Cencek, W., Rychlewski, J., Jaquet, R., & Kutzelnigg, W. 1998, J. Chem. Phys., 108, 2831
Chance, K. V., Park, K., Evenson, K. M., Zink, L. R., Stroh, F., Fink, E. H., & Ramsay, D. A 1997, J. Mol. Spectrosc., 183, 418
Cordonnier, M., Uy, D., Dickson, R. M., Kerr, K. E., Zhang, Y., & Oka, T. 2000, J. Chem. Phys., 113, 3181
Cosby, P. C., & Helm, H. 1988a, Chem. Phys. Lett., 152, 71
Cosby, P. C., & Helm, H. 1988b, Phys. Rev. Lett., 61, 298
Cosby, P. C., & Huestis, D. L. 1992, J. Chem. Phys., 97, 6108
Cotter, R. J., Rozett, R. W., & Koski, W. S. 1972, J. Chem. Phys., 57, 4100
Cox, J. D., Wagman, D. D., & Medvedev, V. A. 1989, CODATA Key Values for Thermodynamics (New York: Hemisphere)
Dodhy, A., Ketterle, W., Messmer, H.-P., & Walther, H. 1988, Chem. Phys. Lett., 151, 133
Dunning, T. H., Jr. 1989, J. Chem. Phys., 90, 1007
Fehsenfeld, F. C., Lindinger, W., & Albritton, D. L. 1975, J. Chem. Phys., 63, 443
Feller, D., & Peterson, K. A. 2007, J. Chem. Phys., 126, 114105
Fennelly, P. F., Hemsworth, R. S., Schiff, H. I., & Bohme, D. K. 1973, J. Chem. Phys., 59, 6405
Frye, D., Preiskorn, A., Lie, G. C., & Clementi, E. 1990, J. Chem. Phys., 92, 4948
Galster, U., Baumgartner, F., Müller, U., Helm, H., & Jungen, M. 2005, Phys. Rev. A, 72, 062506

Galster, U., Kaminski, P., Beckert, M., Helm, H., & Müller, U. 2001, Eur. Phys. J. D, 17, 307
Ganyushin, D., & Neese, F. 2006, J. Chem. Phys., 125, 024103
Goldsmith, P. F., Li, D., Bergin, E. A., Melnick, G. J., Tolls, V., Howe, J. E., Snell, R. L., & Neufeld, D. A. 2002, ApJ, 576, 814
Goldsmith, P. F., et al. 2000, ApJ, 539, L123
Gurvich, L. V., Veyts, I. V., & Alcock, C. B. 1989, Thermodynamic Properties of Individual Substances, Vol. 1, Parts 1 & 2 (New York: Hemisphere)
Gurvich, L. V., Veyts, I. V., & Alcock, C. B. 1991, Thermodynamic Properties of Individual Substances, Vol. 2, Parts 1 & 2 (New York: Hemisphere)
Gurvich, L. V., Veyts, I. V., & Alcock, C. B. 1996, Thermodynamic Properties of Individual Substances, Vol. 3, Parts 1 & 2 (New York: Begell House)
Helm, H. 1988, Phys. Rev. A, 38, 3425
Herbst, E., Green, S., Thaddeus, P., & Klemperer, W. 1977, ApJ, 215, 503
Hiraoka, K., Saluja, P. P. S., & Kebarle, P. 1979, Can. J. Chem., 57, 2159
Ho, W. C., Pursell, C. J., & Oka, T. 1991, J. Mol. Spectrosc., 149, 530
Huang, X., & Lee, T. J. 2008, J. Chem. Phys., 129, 044312
Huber, K. P., & Herzberg, G. 1979, Molecular Spectra & Molecular Structure: IV. Constants of Diatomic Molecules (New York: Van Nostrand Reinhold)
Hunter, E. P., & Lias, S. G. 2005, in NIST Chemistry WebBook, NIST Standard Reference Database Number 69, Proton Affinity Evaluation, ed. P. J. Linstrom & W. G. Mallard (Gaithersburg: National Institute of Standards and Technology),http://webbook.nist.gov
Indriolo, N., Geballe, T. R., Oka, T., & McCall, B. J. 2007, ApJ, 671, 1736
Jaquet, R., Cencek, W., Kutzelnigg, W., & Rychlewski, J. 1998, J. Chem. Phys., 108, 2837
Jaquet, R., & Röhse, R. 1995, Mol. Phys., 84, 291
Karton, A., Rabinovich, E., Martin, J. M. L., & Ruscic, B. 2006, J. Chem. Phys., 125, 144108
Kendall, R. A., Dunning, T. H., Jr., & Harrison, R. J. 1992, J. Chem. Phys., 96, 6796
Ketterle, W., Messmer, H.-P., & Walther, H. 1989, Europhys. Lett., 8, 333
Kim, J. K., Theard, L. P., & Huntress, W. T., Jr. 1975, Chem. Phys. Lett., 32, 610
Knowles, P. J., Hampel, C., & Werner, H.-J. 1993, J. Chem. Phys., 99, 5219
Knowles, P. J., & Werner, H.-J. 1985, Chem. Phys. Lett., 115, 259
Knowles, P. J., & Werner, H.-J. 1988, Chem. Phys. Lett., 145, 514
Kołos, W., & Wolniewicz, L. 1964, J. Chem. Phys., 41, 3663
Kołos, W., & Wolniewicz, L. 1965, J. Chem. Phys., 43, 2429
Kołos, W., & Wolniewicz, L. 1968, J. Chem. Phys., 49, 404
Lacy, J. H., Knacke, R., Geballe, T. R., & Tokunaga, A. T. 1994, ApJ, 428, L69
Larsson, B., et al. 2007, A&A, 466, 999
Le Roy, R. J. 1971, J. Chem. Phys., 54, 5433
Lee, H.-H., Bettens, R. P. A., & Herbst, E. 1996, A&AS, 119, 111
Lie, G. C., & Frye, D. 1992, J. Chem. Phys., 96, 6784
Lindsay, C. M., & McCall, B. J. 2001, J. Mol. Spectrosc., 210, 60
Litorja, M., & Ruscic, B. 1998, J. Electron Spectrosc., 97, 131
Martin, J. M. L., & de Oliveira, G. 1999, J. Chem. Phys., 111, 1843
Mátyus, E., Czakó, G., Sutcliffe, B. T., & Császár, A. G. 2007, J. Chem. Phys., 127, 084102
McCall, B. J. 2006, Philos. Trans. R. Soc. A, 364, 2953
McCall, B. J., Geballe, T. R., Hinkle, K. H., & Oka, T. 1999, ApJ, 522, 338
Meyer, D. M., & Roth, K. C. 1991, ApJ, 376, L49
Neese, F. 2007, J. Chem. Phys., 127, 164112
Neese, F. 2008, ORCA, An Ab Initio, Density Functional, and Semiempirical Program Package, version 2.6, Rev. 35 (Bonn: Univ. Bonn)
Nizkorodov, S. A., Roth, D., Olkhov, R. V., Maier, J. P., & Dopfer, O. 1997, Chem. Phys. Lett., 278, 26
Oka, T. 2004, J. Mol. Spectrosc., 228, 635
Parthiban, S., & Martin, J. M. L. 2001, J. Chem. Phys., 114, 6014
Polyansky, O. L., Prosmiti, R., Klopper, W., & Tennyson, J. 2000, Mol. Phys., 98, 261
Polyansky, O. L., & Tennyson, J. 1999, J. Chem. Phys., 110, 5056
Quack, M. 1977, Mol. Phys., 34, 477
Quan, D., Herbst, E., Millar, T. J., Hassel, G. E., Lin, S. Y., Guo, H., Honvault, P., & Xie, D. 2008, ApJ, 681, 1318
Ramanlal, J., Polyansky, O. L., & Tennyson, J. 2003, A&A, 406, 383
Robbe, J. M., Monnerville, M., Chambaud, G., Rosmus, P., & Knowles, P. J. 2000, Chem. Phys., 252, 9
Röhse, R., Klopper, W., & Kutzelnigg, W. 1993, J. Chem. Phys., 99, 8830
Röhse, R., Kutzelnigg, W., Jaquet, R., & Klopper, W. 1994, J. Chem. Phys., 101, 2231
Ruscic, B. 2004, in 2005 Yearbook of Science & Technology, Active Thermochemical Tables (New York: McGraw-Hill), 3
Ruscic, B., Pinzon, R. E., Morton, M. L., Srinivasan, N. K., Su, M.-C., Sutherland, J. W., & Michael, J. V. 2006, J. Phys. Chem. A, 110, 6592
Ruscic, B., Pinzon, R. E., von Laszewski, G., Kodeboyina, D., Burcat, A., Leahy, D., Montoya, D., & Wagner, A. F. 2005a, J. Phys. Conf. Ser., 16, 561
Ruscic, B., et al. 2004, J. Phys. Chem. A, 108, 9979
Ruscic, B., et al. 2005b, J. Phys. Chem. Ref. Data, 34, 573, http://www.iupac.org/projects/2003/2003-024-1-100.html
Saito, S., & Matsumura, C. 1980, J. Mol. Spectrosc., 80, 34
Senekowitsch, J. 1988, PhD thesis, Univ. Frankfurt
Sidhu, K. S., Miller, S., & Tennyson, J. 1992, A&A, 255, 453
Srinivasan, N. K., Su, M.-C., Sutherland, J. W., Michael, J. V., & Ruscic, B. 2006, J. Phys. Chem. A, 110, 6602
Tinkham, M., & Strandberg, M. W. P. 1955, Phys. Rev., 97, 937
Tom, B. A., Wiczer, M. B., Mills, A. A., Crabtree, K. N., & McCall, B. J. 2008, 63rd Ohio State Univ. International Symp. on Molecular Spectroscopy (Columbus, OH: Ohio St. Univ.), MI04 http://molspect.chemistry.ohio-state.edu/symposium_63/symposium/Program/MI.html#MI04
Uy, D., Cordonnier, M., & Oka, T. 1997, Phys. Rev. Lett., 78, 3844
Viegas, L. P., Alijah, A., & Varandas, A. J. C. 2007, J. Chem. Phys., 126, 074309
Waech, T. G., & Bernstein, R. B. 1967, J. Chem. Phys., 46, 4905
Watts, J. D., Gauss, J., & Bartlett, R. J. 1993, J. Chem. Phys., 98, 8718
Werner, H.-J., & Knowles, P. J. 1985, J. Chem. Phys., 82, 5053
Werner, H.-J., & Knowles, P. J. 1988, J. Chem. Phys., 89, 5803
Werner, H.-J., et al. 2002, MOLPRO: A Package of Ab Initio Programs version 2002.6 (Birmingham: Univ. Birmingham), http://www.molpro.net
Woodall, J., Agúndez, M., Markwick-Kemper, A. J., & Millar, T. J. 2007, A&A, 466, 1197
Woon, D. E., & Dunning, T. H., Jr. 1995, J. Chem. Phys., 103, 4572
Yamada, C., Endo, Y., & Hirota, E. 1983, J. Chem. Phys., 78, 4379